# 2D Phased Arrays

Lucas Åkerstedt, Mika Söderström

July 13, 2022

## 1 Introduction

By creating an antenna consisting of multiple antenna elements, it is possible to radiate in a desired direction by electrically introducing a phase shift to each antenna element. We call this type of antenna, a phased array antenna. In this short piece, we want to show how the geometry of a phased array antenna can alter its performance.

## 2 Theory

When analyzing the behaviour of an antenna, we often need the far-field of the antenna. To obtain the far-field of an antenna, we can utilize the far-field approximation. In this case, we are only using a sum of antenna elements.

We start by deriving the far-field behaviour for an isotropic antenna element. Such an element would radiate a spherical wave:

$$\frac{e^{-jk|\boldsymbol{r}-\boldsymbol{r}'|}}{|\boldsymbol{r}-\boldsymbol{r}'|}, \tag{1}$$

where $r$ is the field vector and $r'$ is the source vector. By assuming a large distance from the antenna ($kr \gg 1$ and $r \gg r'$), we can approximate our spherical wave as following:

$$|\boldsymbol{r}-\boldsymbol{r}'| = \sqrt{(\boldsymbol{r}-\boldsymbol{r}')\cdot(\boldsymbol{r}-\boldsymbol{r}')} = \sqrt{r^2+(r')^2-2\boldsymbol{r}\cdot\boldsymbol{r}'} = r\sqrt{1+\frac{(r')^2}{r^2}-2\frac{\hat{\boldsymbol{r}}\cdot\boldsymbol{r}'}{r}}, \tag{2}$$

expanding the contents under the square root with the small argument Taylor expansion

$$(1+\varepsilon)^p \approx 1+p\varepsilon+\mathcal{O}\left(\varepsilon^2\right) \tag{3}$$

we obtain

$$|\boldsymbol{r}-\boldsymbol{r}'| \approx r\left(1-\frac{\hat{\boldsymbol{r}}\cdot\boldsymbol{r}'}{r}+\frac{1}{2}\frac{(r')^2}{r^2}\right) = r-\hat{\boldsymbol{r}}\cdot\boldsymbol{r}'+\mathcal{O}\left(\frac{1}{r}\right), \tag{4}$$

which yields

$$\frac{e^{-jk|\boldsymbol{r}-\boldsymbol{r}'|}}{|\boldsymbol{r}-\boldsymbol{r}'|} \approx \frac{1}{r}e^{-jkr}e^{jk\hat{\boldsymbol{r}}\cdot\boldsymbol{r}'}. \tag{5}$$

Having a sum of isotropic antenna elements of this kind and neglecting mutual coupling, we can obtain our total field as

$$\sum_{n=1}^{N}\frac{1}{r}e^{-jkr}e^{jk\hat{\boldsymbol{r}}\cdot\boldsymbol{r}'_n} = \frac{1}{r}e^{-jkr}\sum_{n=1}^{N}e^{jk\hat{\boldsymbol{r}}\cdot\boldsymbol{r}'_n} = \frac{1}{r}e^{-jkr}AF, \tag{6}$$

where we have defined our array factor ($AF$) as the contribution from the sum of isotropic antenna elements. For cases where our antenna elements are not isotropic, we add on a factor $E_e$ to obtain the total field

$$\left|F(\theta,\varphi)\right|^2 = \left|E_e(\theta,\varphi)AF(\theta,\varphi)\right|^2 = \left|E_e(\theta,\varphi)\sum_{n=1}^{N}e^{jk\hat{\boldsymbol{r}}\cdot\boldsymbol{r}'_n}\right|^2. \tag{7}$$

By specifying our array geometry we can express the sum in 7 more easily. We define our array as a 2D uniform array consisting of $N$ rows and $M$ columns, placed in the xy-plane, with an element distance $d$:

$$\boldsymbol{r}'_{m,n} = x_m\hat{\boldsymbol{x}} + y_n\hat{\boldsymbol{y}}, \quad x_m = md, \quad y_n = nd. \tag{8}$$

Calculating the scalar product of 7, with the source-vector of 8, we have

$$AF = \sum_{m=0}^{M-1}\sum_{n=0}^{N-1} e^{jk[x_m \sin\theta\cos\varphi + y_n \sin\theta\sin\varphi]}. \tag{9}$$

We also introduce an element unique phase shift $p_{m,n}$ where

$$p_{m,n} = e^{-jk[x_m \sin\theta_0\cos\varphi_0 + y_n \sin\theta_0\sin\varphi_0]}. \tag{10}$$

This yields us

$$AF = \sum_{m=0}^{M-1} p_m e^{jk[x_m \sin\theta\cos\varphi]} \sum_{n=0}^{N-1} p_n e^{jk[y_n \sin\theta\sin\varphi]}. \tag{11}$$

We begin by rewriting the inner sum of 11

$$\sum_{n=0}^{N-1} p_n e^{jk[y_n \sin\theta\sin\varphi]} = \sum_{n=0}^{N-1} e^{jk[nd\sin\theta\sin\varphi - nd\sin\theta_0\sin\varphi_0]} = \sum_{n=0}^{N-1}\left(e^{jkd[\sin\theta\sin\varphi - \sin\theta_0\sin\varphi_0]}\right)^n. \tag{12}$$

Here we can use the geometric series

$$\sum_{n=0}^{N-1} ax^n = a + ax + ... + ax^{N-1} = a\frac{x^N - 1}{x - 1}, \tag{13}$$

which yields us

$$\begin{aligned}\sum_{n=0}^{N-1}\left(e^{jkd[\sin\theta\sin\varphi - \sin\theta_0\sin\varphi_0]}\right)^n = \sum_{n=0}^{N-1}\left(e^{j[\psi-\psi_0]}\right)^n = \frac{e^{jN[\psi-\psi_0]}-1}{e^{j[\psi-\psi_0]}-1} = \\ \frac{e^{j\frac{N}{2}[\psi-\psi_0]}}{e^{j\frac{[\psi-\psi_0]}{2}}}\left[\frac{e^{j\frac{N}{2}[\psi-\psi_0]} - e^{-j\frac{N}{2}[\psi-\psi_0]}}{e^{j\frac{[\psi-\psi_0]}{2}} - e^{-j\frac{[\psi-\psi_0]}{2}}}\right] = \frac{e^{j\frac{N}{2}[\psi-\psi_0]}}{e^{j\frac{[\psi-\psi_0]}{2}}}\left[\frac{2j\sin\left(\frac{N}{2}[\psi-\psi_0]\right)}{2j\sin\left(\frac{1}{2}[\psi-\psi_0]\right)}\right] = \\ e^{j[\psi-\psi_0](\frac{N-1}{2})}\frac{\sin\left(\frac{N}{2}[\psi-\psi_0]\right)}{\sin\left(\frac{1}{2}[\psi-\psi_0]\right)},\end{aligned} \tag{14}$$

where $\psi = kd\sin\theta\sin\varphi$ and $\psi_0 = kd\sin\theta_0\sin\varphi_0$. For the outer sum of 11, we perform the same operations as was done in 14. This yields us

$$AF = e^{j[\psi-\psi_0](\frac{N-1}{2})}e^{j[\zeta-\zeta_0](\frac{M-1}{2})}\frac{\sin\left(\frac{N}{2}[\psi-\psi_0]\right)}{\sin\left(\frac{1}{2}[\psi-\psi_0]\right)}\frac{\sin\left(\frac{M}{2}[\zeta-\zeta_0]\right)}{\sin\left(\frac{1}{2}[\zeta-\zeta_0]\right)}, \tag{15}$$

where $\zeta = kd\sin\theta\cos\varphi$ and $\zeta_0 = kd\sin\theta_0\cos\varphi_0$. From the acquired expression, it is clear that the maximum array factor $AF$ is in the direction $\hat{\boldsymbol{r}}(\theta_0, \varphi_0)$. However, one can also see that if $kd$ is large enough, there will be multiple maximums over the unit sphere.

We can further calculate the directivity $D$ of the array factor

$$D(\theta,\varphi) = \frac{4\pi|AF(\theta,\varphi)|^2}{\int_\Omega |AF|^2 d\Omega}. \tag{16}$$

The integral in the denominator of 16 is given by

$$\int_0^{2\pi}\int_0^{\pi}\left|\frac{\sin\left(\frac{N}{2}[\psi-\psi_0]\right)}{\sin\left(\frac{1}{2}[\psi-\psi_0]\right)}\frac{\sin\left(\frac{M}{2}[\zeta-\zeta_0]\right)}{\sin\left(\frac{1}{2}[\zeta-\zeta_0]\right)}\right|^2 \sin\theta d\theta d\varphi. \tag{17}$$

# 3 Array geometries

## 3.1 Basic geometries

We start by analyzing a standard phased array geometry: the four-by-four uniform phased array (see Figure 1).

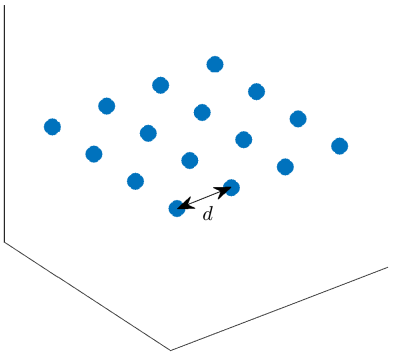


Figure 1: Uniform four-by-four array with distance $d$ between the elements.

By using the geometry suggested in Figure 1 and operating on a frequency such that the uniform element distance $d$ corresponds to $\lambda/2$, where $\lambda$ is the wavelength, we get a far-field pattern calculated from the array factor $AF$, that can be seen in Figure 2 (a). Furthermore we can see the complete shape of the far-field in relation to the antenna elements in Figure 2 (b).

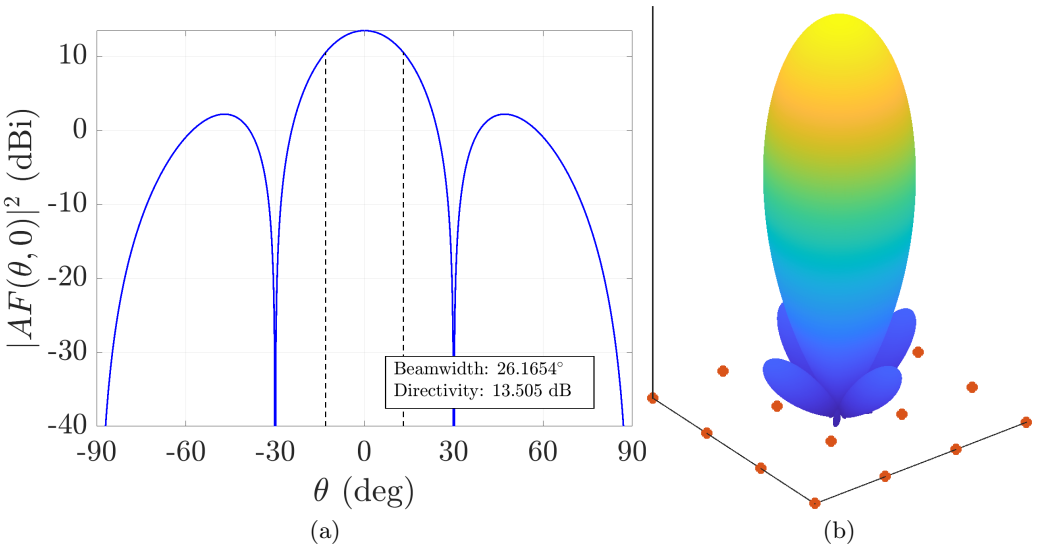


Figure 2: The far-field of the four-by-four array, with a uniform distance $d$ corresponding to $\lambda/2$ in (a). The three-dimensional far-field pattern of the four-by-four array in (b).

By extending the uniform element distance $d$ such that it now corresponds to $\lambda$, we get an interesting result, seen in Figure 3. We now get what is called grating lobes. These grating lobes are sidelobes that have the same gain as the mainbeam, although in another direction. However, the mainbeam beamwidth is smaller then for the array with a uniform element distance of $\lambda/2$.

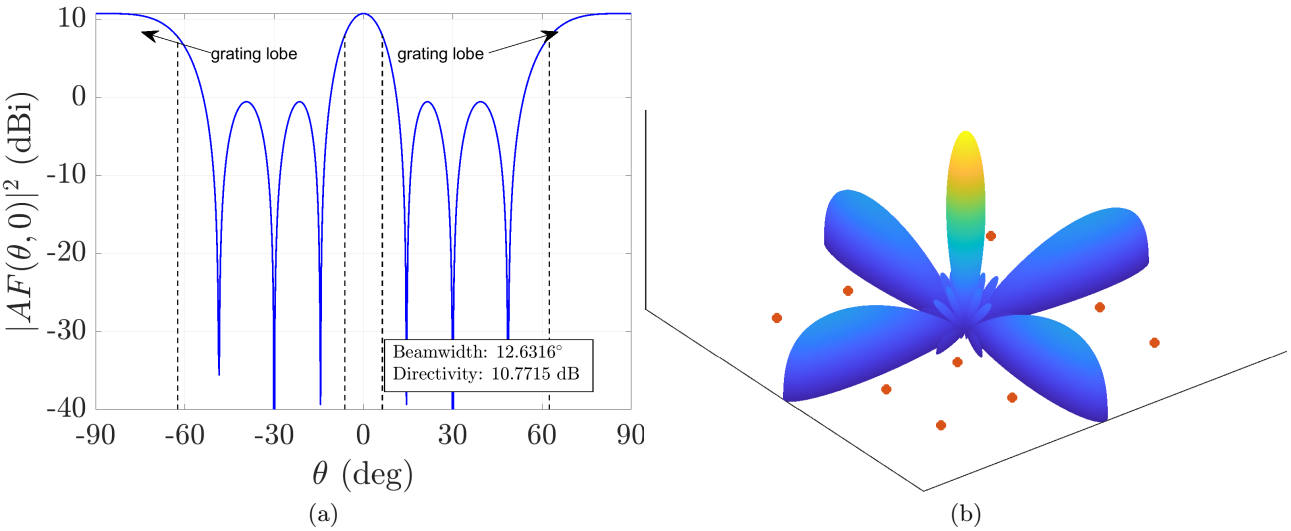


Figure 3: The far-field of the four-by-four array, with a uniform distance $d$ corresponding to $\lambda$ in (a). The three-dimensional far-field pattern of the four-by-four array in (b).

Then lastly, if we decrease the unifrom element distance to $\lambda/4$ we get the result seen in Figure 4.

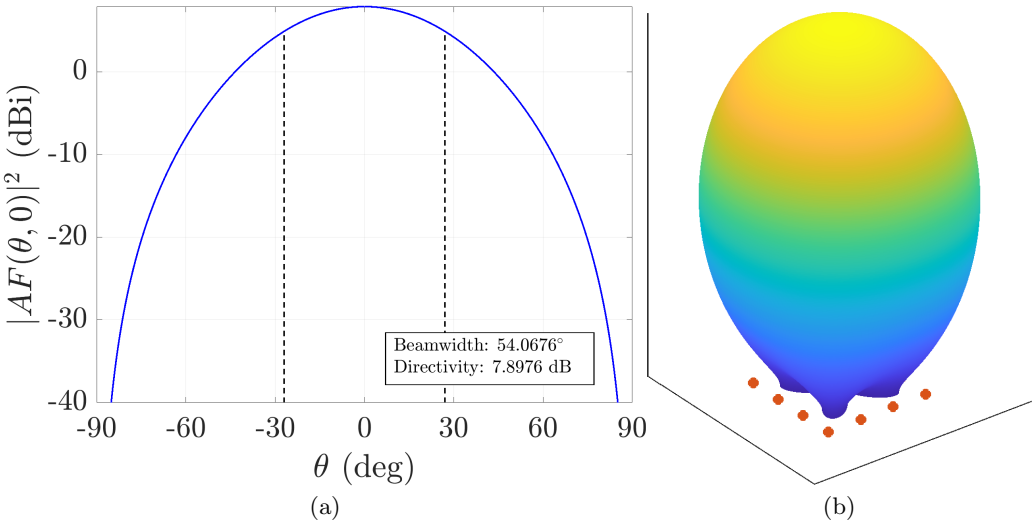


Figure 4: The far-field of the four-by-four array, with a uniform distance $d$ corresponding to $\lambda/4$ in (a). The three-dimensional far-field pattern of the four-by-four array in (b).

### 3.2 Adaptive array configuration

As explained in the previous section, the element distance has a large impact on the far-field of the array. We saw that extending the distance between the elements can increase the beamwidth (and for some cases the directivity), but increase it too much and there will appear grating lobes. When working on small band arrays, one typically wants to have the distance between the elements to be around $\lambda/2$ if one wants to maximize the directivity and avoid grating lobes. For wideband arrays, however, there is a problem that one will run in to after a while.

For a wideband uniform 2D phased array system where the objective is to have the highest directivity possible, the first step would be to design the uniform element distance after the wavelength corresponding to the highest frequency of the intended band. This would ensure a very high directivity for the upper frequencies of the intended band. For the lower frequencies the element distance appear as a very small distance in terms of the lower frequencies wavelengths. This means the directivity for the lower frequencies gets lower than the directivity for the higher frequencies. It is however possible to expand the distance between the elements by not using them. By ignoring a well chosen group of array elements, the distance between them can appear longer, however at the cost of using fewer elements. We can thus reconfigure our phased array system to maintain

a higher directivity at lower frequencies. To do this, we have defined a couple of "configuration modes" that determines which array element to disable (in this case for an eight-by-eight array, see Figure 5).

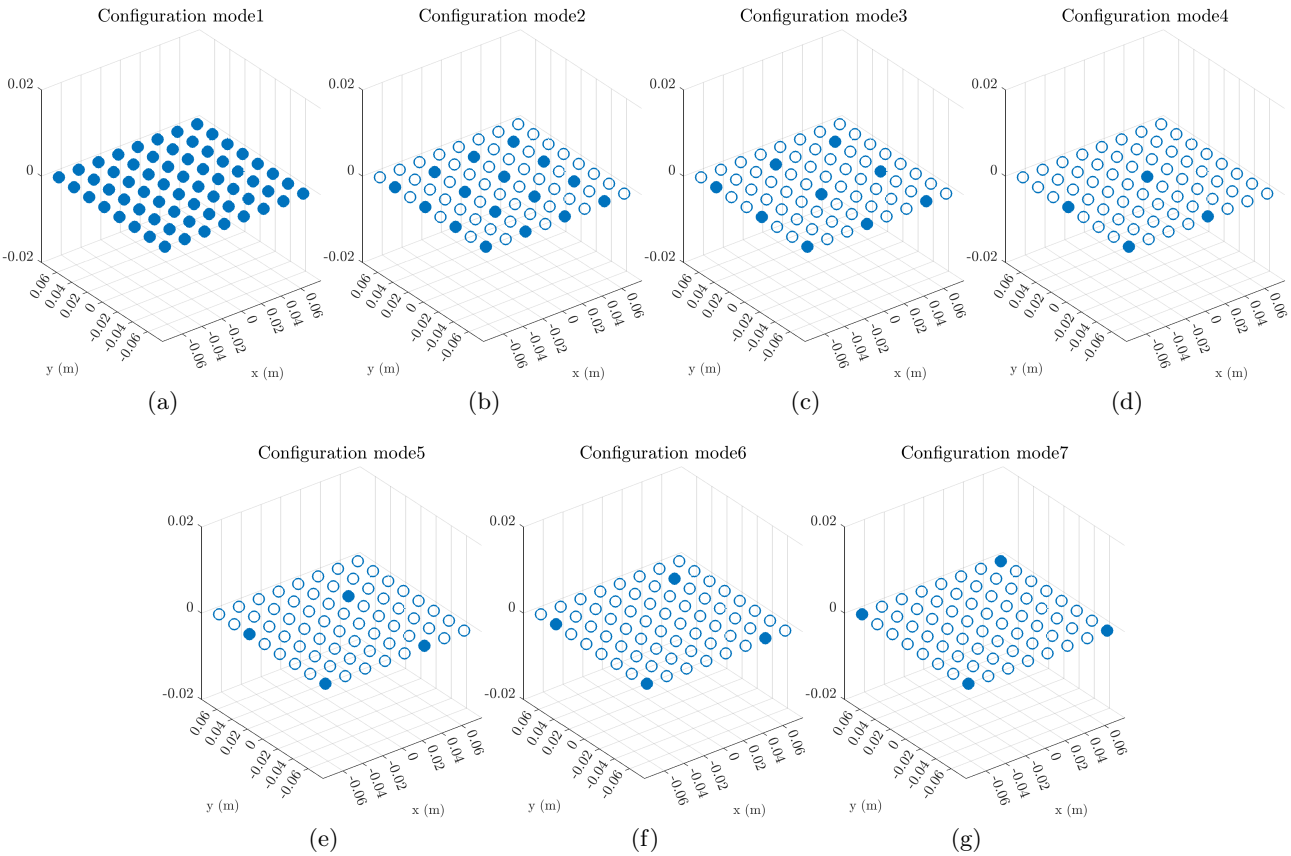


Figure 5: The different configuration modes for an eight-by-eight uniform array, where a solid circle indicates an array element in use and a circle with white face color indicates an array element not in use.

We can test these configuration modes out by creating an eight-by-eight uniform array with an element distance $d$ of 20 mm. This corresponds roughly to $\lambda/2$ for the frequency 8.5 kHz (for a wave velocity of 343 m/s). We can then calculate the broadside directivity of the array at an operating frequency of 1.2 kHz. This yields us the result seen in Figure 6.

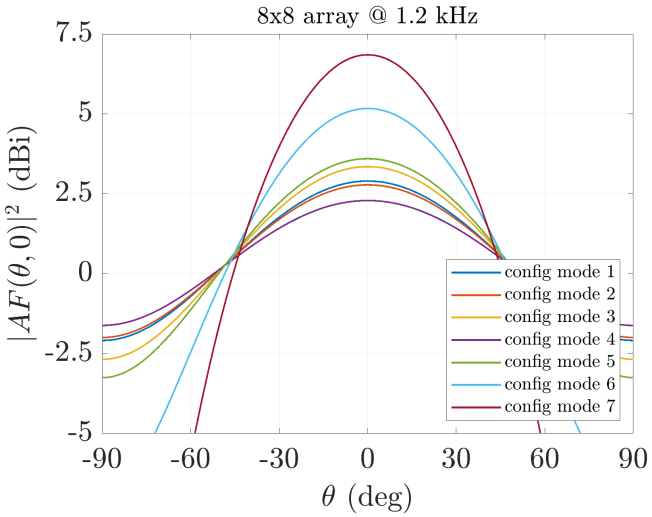


Figure 6: Uniform four-by-four array with distance $d$ between the elements.

As can be seen in Figure 6, it is more beneficial to use the configuration mode 7 to obtain the highest directivity at 1.2 kHz. It is however important to notice that the drawback of this method is that the absolute

gain is lower when disabling array elements. If one is only interested in the magnitude of the signal, then it is always beneficial to using all of the array elements. If the objective however is to have the largest contrast of the incoming signal with dependence of the direction, then it is beneficial to use the configuration modes.

For the same array system used for Figure 6, we can test for multiple frequencies to see how much we can increase the directivity by using the configuration modes. Doing so, we must add one constraint. When disabling array elements to enlarge the element distance, we can not enlarge it to a point where the distance becomes larger than $\lambda/2$ for the intended frequency. The result for the proposed test can be seen in Figure 7

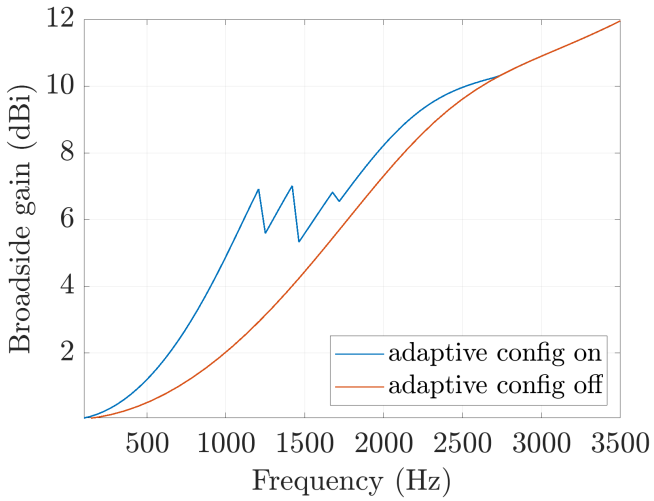


Figure 7: The broadside gain of the eight-by-eight uniform array for frequencies from 100 - 3500 Hz, with adaptive configuration and without adaptive configuration.

To know which configuration mode will give the highest directivity for a given frequency, one must try all the eligible configuration modes. This means that the directivity of the array system using one specific configuration mode must be calculated. To then integrate this solution to a system, one must either be able to calculate the integral given in 17 fast, or do all of the calculations beforehand. Furthermore, the suggested configuration modes in Figure 5 may not be the configuration modes that can yield the highest directivity for a given frequency. There can be a lot of patterns realized on the eight-by-eight grid, but one of the patterns will yield the highest directivity in a given direction for a given frequency.

### 3.3 Multiple arrays

We can use multiple arrays placed in a certain manner to obtain different kind of far-field patterns. The easiest way of placing these arrays would be the same way we placed our antenna elements; uniformly. Such a placement of arrays can be seen in Figure 8.

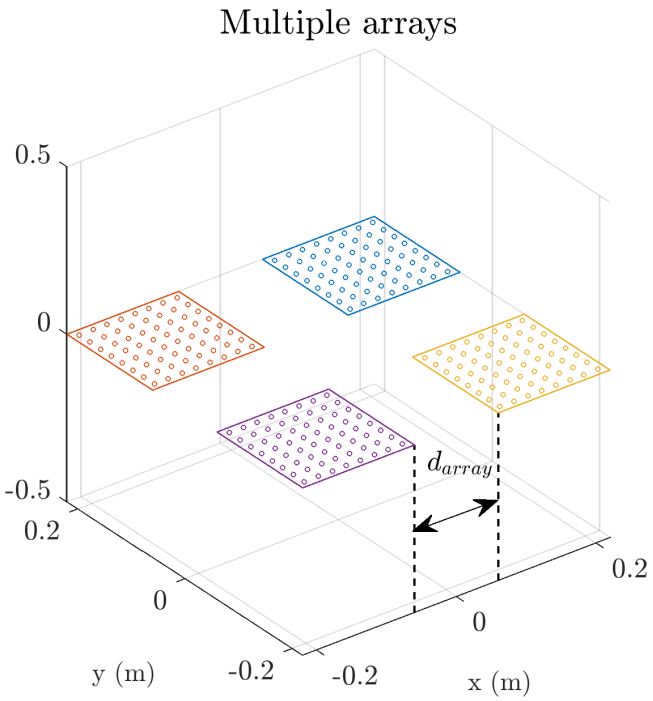


Figure 8: Multiple arrays with a uniform distance $d_{array}$ from each other.

By adjusting this array distance $d_{array}$, we can get different far-field patterns. These far-field patterns can be seen in Figure 9.

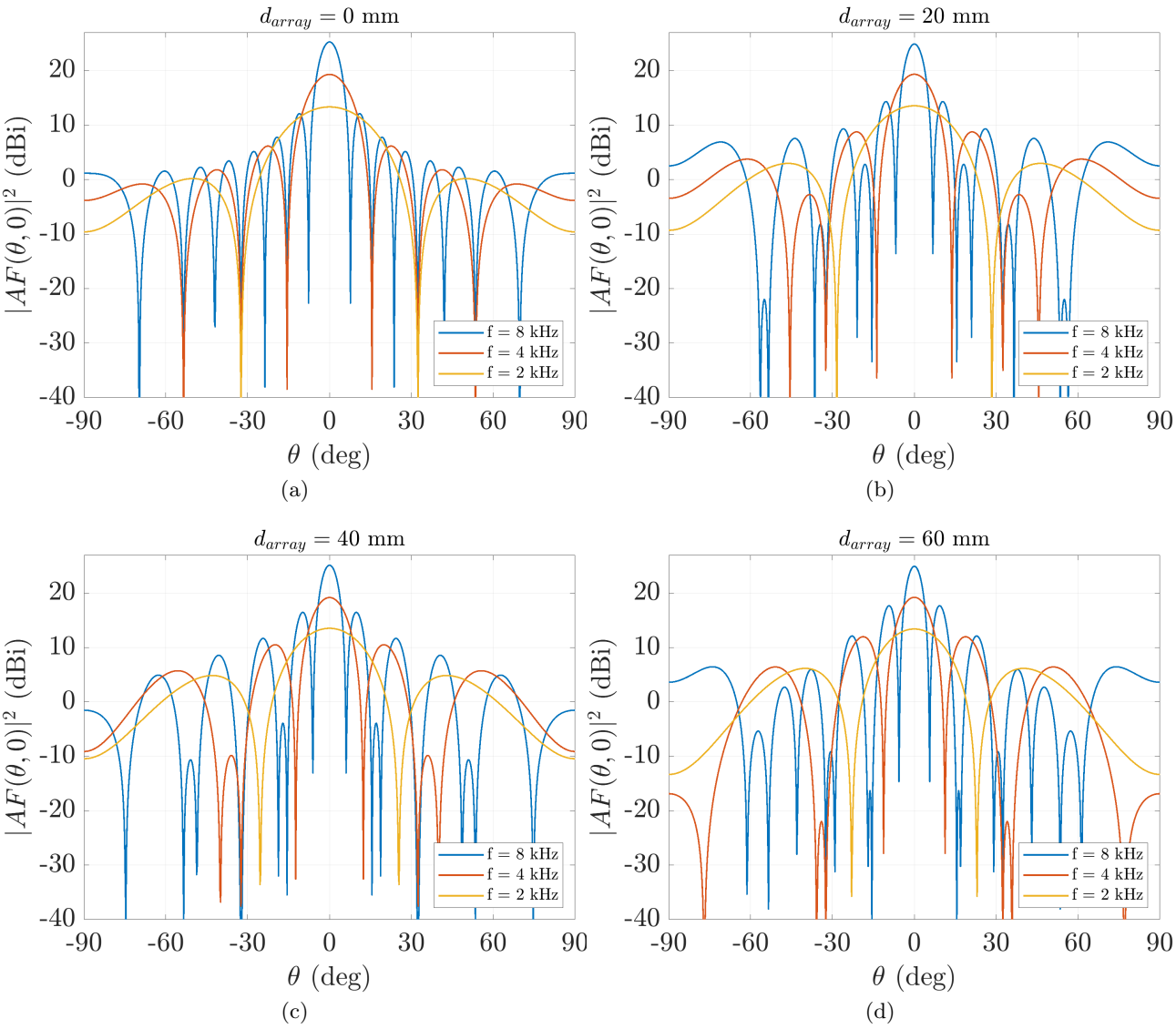


Figure 9: The different far-field patterns of a system consisting of four eight-by-eight arrays, with a uniform array distance of 0 mm in (a), 20 mm in (b), 40 mm in (c), and 60 mm in (d).

### 3.4 Multiple arrays with adaptive array configuration

Combining adaptive array configuration with multiple array antennas yields interesting results. We will however only use the simple configuration modes derived earlier. Also since adaptive array configuration yields distinguishable results at lower frequencies from not using adaptive array configuration, lower frequencies will be investigated more than higher frequencies. For four eight-by-eight arrays with a uniform array distance $d_{array}$ of 60 mm, we get the configuration modes as seen in Figure 10.

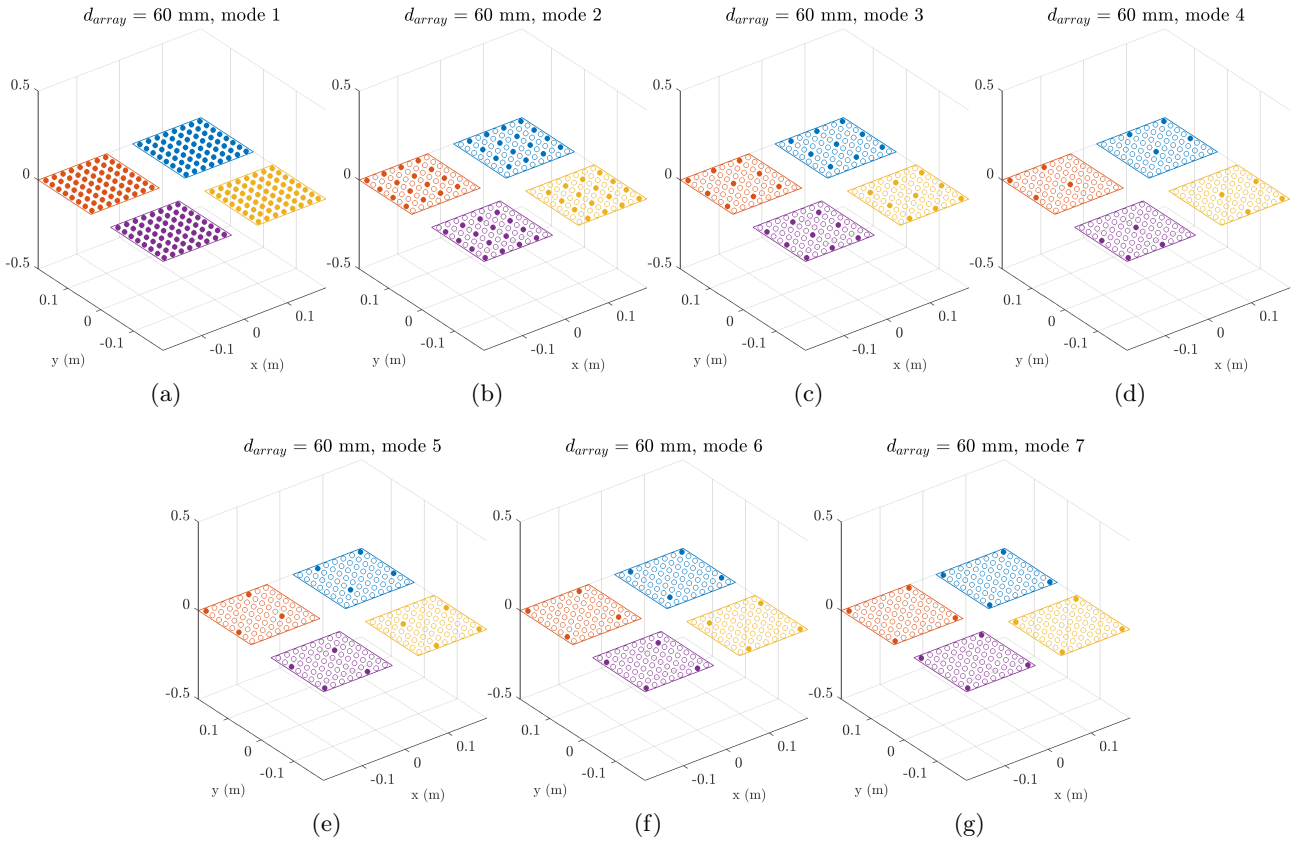


Figure 10: The different configuration modes for four eight-by-eight uniform array with an array distance $d_{array}$ of 60 mm, where a solid circle indicates an array element in use and a circle with white face color indicates an array element not in use.

Operating the four eight-by-eight arrays at 2000 Hz yields the far-field pattern seen in Figure 11.

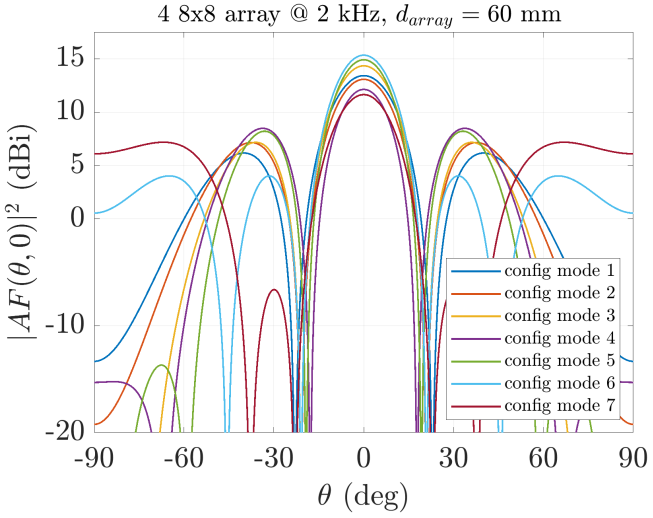


Figure 11: The far field of the four eight-by-eight arrays when using different configuration modes.